boundary condition is $u_i|_\Gamma = E_z|_\Gamma = 0$. From formulations (1), (2), and (3), the cutoff frequencies $f_c(\lambda_c)$ of finline can be determined by the same way as described in [11].

REFERENCES

1. P.J. Meier, Integrated fin-line millimeter components, IEEE Trans Microwave Theory Tech MTT-22 (1974), 1209–1216.
2. A.M.K. Saad and K. Schunemann, A simple method for analyzing fin-line structures, IEEE Trans Microwave Theory Tech MTT-26 (1978), 1002–1007.
3. J.B. Knorr and P.M. Shayda, Millimeter-wave fin-line characteristics, IEEE Trans Microwave Theory Tech MTT-28 (1980), 737–743.
4. A.M.K. Saad and K. Schunemann, Closed-form approximations for fin-line eigenmodes, Proc Inst Elect Eng Pt-H 129 (1982), 253–261.
5. A.K. Sharma and W.J.R. Hoefer, Empirical expressions for fin-line design, IEEE Trans Microwave Theory Tech MTT-31 (1983), 350–356.
6. C.A. Olley and T.E. Rozzi, Systematic characterization of the spectrum of unilateral finline, IEEE Trans Microwave Theory Tech MTT-34 (1986), 1147–1156.
7. T. Rozzi, L. Pierantoni, and M. Farina, Eigenvalue approach to the efficient determination of the hybrid and complex spectrum of inhomogeneous, closed waveguide, IEEE Trans Microwave Theory Tech MTT-45 (1997), 345–352.
8. S. Palanichamy, A. Biswas, and R.K. Shukla, Full-wave analysis of dominant and higher order modes in microstrip-slot coupled line with uniaxial anisotropic dielectric substrates, Microwave Opt Technol Lett 25 (2000), 400–406.
9. Q. Zheng et al., Solution of two-dimensional Helmholtz equation by multipole theory method, J Electromag Waves Appl 13 (1999), 205–220.
10. Q. Zheng et al., Application of the multipole theory method to the analysis of waveguides with sharp metal edges, Microwave Opt Technol Lett 28 (2001), 101–105.
11. Q. Zheng et al., Multipole theory analysis of cutoff wavenumbers of waveguides partially filled with dielectric, Microwave Opt Technol Lett 25 (2000), 397–400.

MEASUREMENT OF DIELECTRIC AND RADIATION LOSSES FOR FLEXIBLE CIRCULAR DIELECTRIC WAVEGUIDES IN Q-BAND

Ki Young Kim,[1] Heung-Sik Tae,[1] and Jeong-Hae Lee[2]
[1] School of Electronic and Electrical Engineering,
Kyungpook National University,
702-701, Daegu, Korea
[2] Radio Science and Communication Engineering,
Hongik University,
Seoul, 121-791, Korea

Received 4 April 2002

ABSTRACT: *Experimental results are presented for the dielectric and radiation losses from flexible circular PTFE waveguides in the Q-band. The dielectric and radiation losses from rod and tube waveguides were found to depend strongly on the design parameters, such as the operating frequency, area of the dielectric region in the guiding cross sections, and curvature radii of the bending. The dielectric losses from the straight guides showed a relatively good agreement with the theoretical results. The radiation losses with a small curvature radius, which cannot be predicted using current theories, were determined based on the differences between the measured insertion losses and the dielectric losses. The validity of the current results was confirmed based on the fractional power flow ratios in each region of the waveguides.* © 2002 Wiley Periodicals, Inc. Microwave Opt Technol Lett 35: 102–106, 2002; Published online in Wiley InterScience (www.interscience.wiley.com). DOI 10.1002/mop.10529

Key words: *flexible waveguide; Q-band; dielectric loss; radiation loss; curvature radius of bend*

1. INTRODUCTION

Various flexible wave-guiding structures have already been extensively studied in an optical frequency range. However, research on a flexible waveguide in a millimeter wave frequency, especially on a dielectric flexible waveguide, has received relatively little attention, although much research has focused on the development of low-loss millimeter wave guiding structures using a dielectric medium [1]. A flexible dielectric guiding structure applicable to a millimeter wave band has various potential applications, including a homo-dyne phase measurement system [2] or millimeter wave MMIC testing system [3–4]. A dielectric rod or tube waveguide is a promising candidate as a low-cost flexible guiding structure in a millimeter wave band, because its loss characteristic is lower than that of a metal flexible waveguide with corrugation [5]. In addition, the mechanical properties of some commercial polymer dielectrics, such as polystyrene, polyethylene, polypropylene, and PTFE [6], are very flexible. Nonetheless, when a dielectric guide is used as a flexible waveguide, an additional radiation loss is generated at the bending section. The phase velocity of the guided waves along the curved section of dielectric waveguides exceeds the velocity of light at a certain distance from the curvature center. Thereafter, the waves are no longer guided and their energy radiates into free space [7].

To determine the exact radiation loss from a curved dielectric waveguide, the electromagnetic fields redistributed at the curved section of the guides, relative to a straight reference guide, needs to be known in advance. Unfortunately, it is very difficult to directly analyze and describe the redistributed fields caused by the bend [8]. It is expected that the redistributed electromagnetic fields at the curved section depend strongly on the design parameters, such as the operating frequency, curvature radius of the bend, and structure of the waveguide, including the dielectric property. However, there is no systematic study on such parameters. Furthermore, previous results from various flexible dielectric waveguides in millimeter wave frequencies have been limited to specific cases [9–11]. For example, the radiation loss was determined in the regime of large curvature radius. For a flexible dielectric waveguide to be utilized practically in a millimeter wave circuit system, the total amount of power radiated from the bent dielectric guiding structure needs to be systematically investigated with the wide range of design parameters.

Accordingly, the present work measured the insertion losses to obtain the dielectric and radiation losses of circular PTFE waveguides in the Q-band (33 GHz to 50 GHz) according to variations in certain parameters, such as the frequency and guiding cross section. In particular, the measurements were performed with large variations of curvature at bend. The dielectric and radiation losses are then qualitatively explained based on the fractional power flows in each region of the guides.

2. FIELD EXPRESSION AND EIGENVALUE EQUATION

Figure 1 shows the geometry of the dielectric waveguides employed in the current study. The wave propagates along the z-direction. The radius of the rod is r, whereas the inner and outer radii of the tube are, r_1 and r_2, respectively. The surrounding media in the rod and tube waveguides, including the hollow region

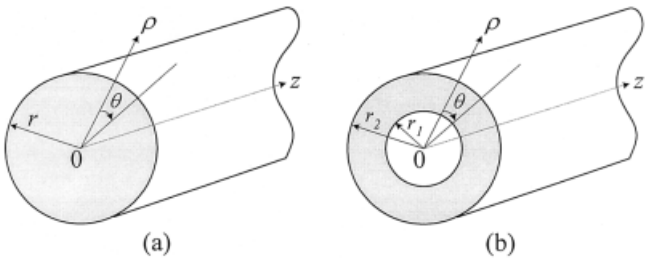

Figure 1 Geometry of circular dielectric waveguides. (a) rod waveguide (b) tube waveguide

from the origin to r_1, are the free spaces. The axial field components of each region of the rod and tube waveguides can be expressed by Eqs. (1)–(4) and (5)–(10), respectively [12–13].

$$E_{zd} = A_m J_m(k_d\rho),\ 0 < \rho < r \tag{1}$$

$$H_{zd} = B_m J_m(k_d\rho),\ 0 < \rho < r \tag{2}$$

$$E_{zf} = C_m K_m(k_f\rho),\ \rho > r \tag{3}$$

$$H_{zf} = D_m K_m(k_f\rho),\ \rho > r \tag{4}$$

$$E_{zi} = A_m I_m(k_i\rho),\ 0 < \rho < r_1 \tag{5}$$

$$H_{zi} = B_m I_m(k_i\rho),\ 0 < \rho < r_1 \tag{6}$$

$$E_{zd} = C_m J_m(k_d\rho) + D_m Y_m(k_d\rho),\ r_1 < \rho < r_2 \tag{7}$$

$$H_{zd} = E_m J_m(k_d\rho) + F_m Y_m(k_d\rho),\ r_1 < \rho < r_2 \tag{8}$$

$$E_{zf} = G_m K_m(k_f\rho),\ \rho > r \tag{9}$$

$$H_{zf} = H_m K_m(k_f\rho),\ \rho > r \tag{10}$$

The propagation factors of $\cos m\theta \exp[j(\omega t - \beta z)]$ (or $\sin m\theta \exp[j(\omega t - \beta z)]$) for the electric fields and $\sin m\theta \exp[j(\omega t - \beta z)]$ (or $\cos m\theta \exp[j(\omega t - \beta z)]$) for the magnetic fields are abbreviated. J_m and Y_m are mth order Bessel functions of the first and second kind; I_m and K_m are modified mth order Bessel functions of the first and second kind. m is the azimuthal eigenvalue. $k_x(x = d, i, f)$ is the propagation constant of the radial direction and is expressed as in Eq. (11)–(13).

$$k_d = k_0\sqrt{\mu_{rd}\varepsilon_{rd} - \bar{\beta}^2} \tag{11}$$

$$k_i = k_0\sqrt{\bar{\beta}^2 - \mu_{ri}\varepsilon_{ri}} \tag{12}$$

$$k_f = k_0\sqrt{\bar{\beta}^2 - \mu_{rf}\varepsilon_{rf}} \tag{13}$$

The subscripts d, i, and f represent the dielectric medium, hollow free space region inside the tube, and outer free space region, respectively. k_0 is the free space wave number, whereas $\bar{\beta}(= \beta/k_0)$ is the normalized propagation constant. μ_{rx} and ε_{rx} are the relative permeability and relative permittivity of each region, respectively. A_m to H_m are the magnitude coefficients of the fields corresponding to the azimuthal eigenvalue. The azimuthal components of the fields are obtained from the axial field components. Equating the tangential field components at the boundaries ($\rho = r$ for the rod waveguides; $\rho = r_1$ and $\rho = r_2$ for the tube waveguides) produces square matrices (4×4 for the rod waveguides and 8×8 for the tube waveguides) for the magnitude coefficients. To obtain an eigenvalue equation, whereby the dispersion relation and field distribution in the cross section of the guide can be determined, the determinant of the coefficient matrix should be set to vanish. The dielectric constant of the dielectric material, radius of the guide, and thickness of the dielectric region for the tube waveguide are all considered as the design parameters in the dispersion relation.

3. DESIGN OF SINGLE MODE WAVEGUIDE

In addition to its dispersion characteristics, the design of a flexible dielectric waveguide in a millimeter wave band requires the consideration of its mechanical properties, such as flexibility for a freely bending waveguide and stability to prevent deformation. In general, dielectrics tend to be hard and rigid as they have higher dielectric constants. Thus, in this study, PTFE was chosen as the guiding medium, as its dielectric constant in the Q-band was assumed to be 2.08 [6]. For a single mode operation, the second mode cutoff also needs to be determined. The fundamental mode of a circular dielectric waveguide is traditionally referred to as the HE_{11} mode, which has no cutoff. Accordingly, when considering both the flexibility and the dispersion properties of the PTFE guides, the outer radii of the guides were set at 2.5 mm (r for the rod and r_2 for the tubes), while the inner radii of the tube waveguide were set at 1.0 mm and 1.5 mm from the dispersion relation [12]. The thickness of the tube with an inner radius of 1.5 mm, was set at 1.0 mm to avoid any deformation when the tube was bent or exposed to an external force.

Figure 2 illustrates the dispersion curve for the waveguides used in the current work. The vertical axis represents the normalized propagation constants. As shown in Figure 2, the second mode cutoff frequency for the rod waveguide with a radius of 2.5 mm was 44.3 GHz. The second (TM_{01} mode) and third mode (TE_{01} mode) cutoff frequencies of the rod waveguide were nearly same. The second mode (TE_{01} mode) cutoff frequencies of the tubes with inner radii of 1.0 mm and 1.5 mm were 45.45 GHz and 49.7 GHz, respectively. With a decrease in the thickness ($r_2 - r_1$) of the tubes, the cutoff frequencies of the second mode shifted toward a higher frequency regime. Based on the selection of PTFE as the guiding material and the above radii in the guiding cross section, the guides could be operated in a single mode for a considerable portion of the Q-band.

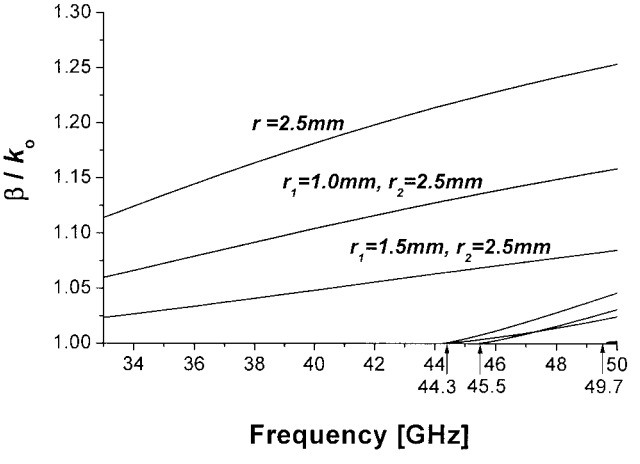

Figure 2 Dispersion curves of various circular PTFE waveguides

4. FRACTIONAL POWER CONSIDERATIONS

The dielectric and radiation losses strongly depend on the amount of power propagated along the dielectric region and outer free space region, respectively, implying that the more power confined in the dielectric region the higher the dielectric loss and the lower the radiation loss, as less power is radiated at the bend. Therefore, the power propagated in each region needs to be investigated relative to the design parameters in order to predict the dielectric and radiation losses. The total power propagated along the rod or tube waveguide, P_T, is expressed in Eqs. (14) and (15), respectively.

$$P_T = \frac{1}{2}\int_0^r (E_{\rho d}H_{\theta d}^* - E_{\theta d}H_{\rho d}^*)\rho d\ \rho + \frac{1}{2}\int_r^\infty (E_{\rho f}H_{\theta f}^* - E_{\theta f}H_{\rho f}^*)\rho d\ \rho \quad \text{for rod waveguide} \quad (14)$$

$$P_T = \frac{1}{2}\int_0^{r_1} (E_{\rho i}H_{\theta i}^* - E_{\theta i}H_{\rho i}^*)\rho d\ \rho + \frac{1}{2}\int_{r_1}^{r_2} (E_{\rho d}H_{\theta d}^* - E_{\theta d}H_{\rho d}^*)\rho d\ \rho + \frac{1}{2}\int_{r_2}^\infty (E_{\rho f}H_{\theta f}^* - E_{\theta f}H_{\rho f}^*)\rho d\ \rho \quad \text{for tube waveguide} \quad (15)$$

In Eqs. (14) and (15), the azimuthal field components are given in (1)–(10). The fractional power flow ratios in each region of the waveguides are defined as follows:

$$P_d = \left\{\frac{1}{2}\int_{\text{Dielectric Region}} (E_{\rho d}H_{\theta d}^* - E_{\theta d}H_{\rho d}^*)\rho\, d\rho\right\}/P_T \quad (16)$$

$$P_i = \left\{\frac{1}{2}\int_0^{r_1} (E_{\rho i}H_{\theta i}^* - E_{\theta i}H_{\rho i}^*)\rho\, d\rho\right\}/P_T \quad (17)$$

$$P_f = \left\{\frac{1}{2}\int_{r \text{ or } r_2}^\infty (E_{\rho f}H_{\theta f}^* - E_{\theta f}H_{\rho f}^*)\rho\, d\rho\right\}/P_T \quad (18)$$

where P_d, P_i, and P_f are the fractional powers propagated in the dielectric region of the rod or tube waveguide, in the inner free space region of the tube waveguide, and in the outer free space of the rod or tube waveguide, respectively.

The fractional power flow ratios in each region of the PTFE waveguides relative to the operating frequency are shown in Figure 3. The fractional power flows are expressed as a function of Bessel functions, whose arguments are related to the design parameters. Consequently, the general relationships between the fractional power flows and the design parameters are quite complicated. In this work, the fractional power flows were obtained relative to the frequencies from 33 GHz to 50 GHz. Figure 3(a) shows that the propagating powers in the dielectric region increased with an increase in both the frequency and the dielectric area. For the tube guides, the fractional power flows in the free space region inside the tube increased with an increase in the

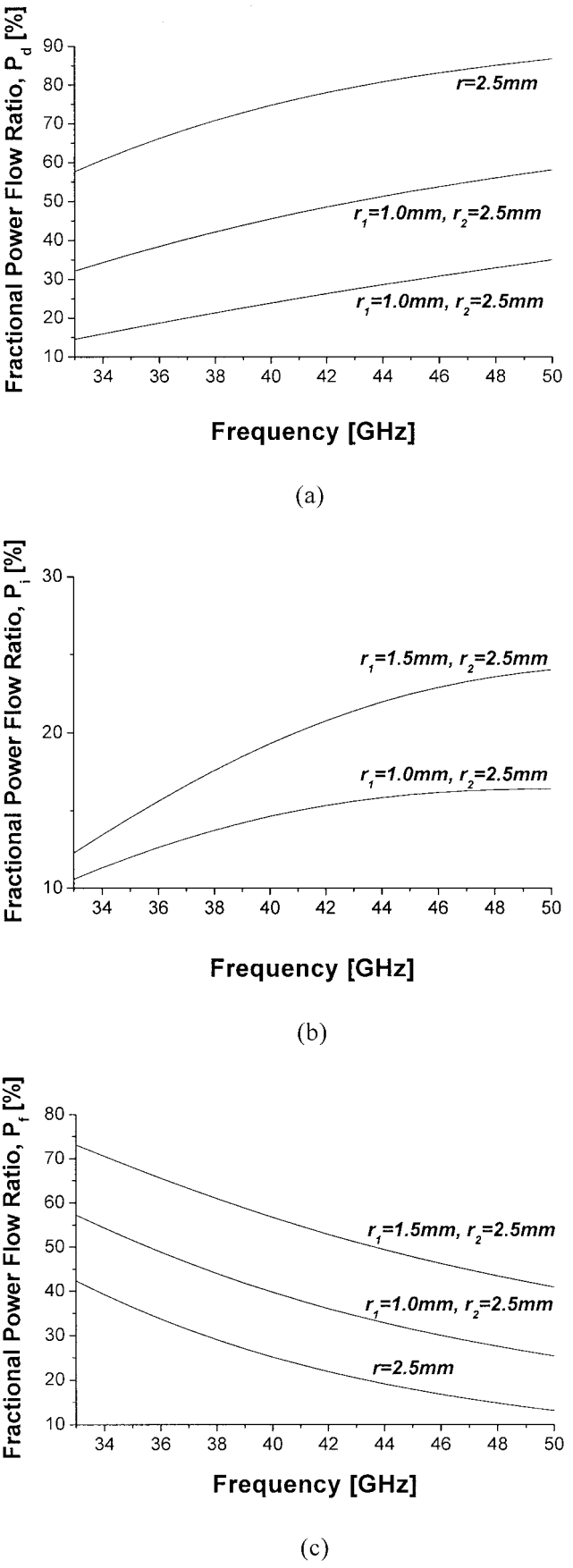

Figure 3 Fractional power flow ratios in each region of PTFE waveguides: (a) dielectric region (b) air core region (c) free space region

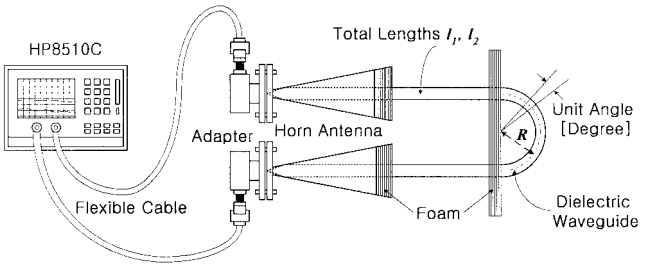

Figure 4 Experimental setups

frequency, whereas they decreased with an increase in the dielectric areas, as shown in Figure 3(b). In Figure 3(c), the amount of power propagated along the outside of the rod or tube waveguide was found to decrease relative to an increase in the operating frequency and dielectric area. These fractional power flows are used to explain both the dielectric and radiation losses in a later section.

5. MEASUREMENTS

Figure 4 illustrates a schematic diagram of the experimental setup used to take the measurements. The experiments were performed with an HP8510C vector network analyzer (VNA) to obtain scattering parameters. Two 25 dBi standard gain horn antennas were used to efficiently launch and receive the signals from the vector network analyzer. The PTFE guides were inserted into the horn antennas, as illustrated in Figure 4. The central position in the horn and semicircle shape of the bending section of the guide were fixed with foam. Both tips of the rod waveguides were tapered to reduce the return loss, achieving approximately below −20 dB. The return losses of the tube waveguides were also below −20 dB without any tapering. To determine the attenuations per unit length of the straight PTFE guide, the insertion losses of various samples with different lengths and the same bending sections were measured relative to an operating frequency from 33 GHz to 50 GHz. The specifications of the samples used in this measurement are shown in Table 1.

The radiation characteristics of the two guides with the same curvature radius were assumed to be same, even though they had different lengths. Consequently, the dielectric loss α_d representing the attenuations per wavelength for the straight rod and tube waveguides was obtained using Eq. (19).

$$\alpha_d = -\frac{10\,\mathrm{Log}_{10}[1-(10^{S_{21,l_2}/10}-10^{S_{21,l_1}/10})]}{l_1-l_2}\frac{1}{F}\,[dB/\lambda_g] \quad (19)$$

In Eq. (19), F is a dimensionless factor transforming dB/cm to dB/λ_g, that is, $30/f\sqrt{\varepsilon_r}$ where the frequency f is in GHz, and, the guided wavelength, λ_g is in cm. S_{21,l_1} and S_{21,l_2} are the measured insertion losses of the samples with different lengths, l_1 and l_2, at

TABLE 1 Total Lengths and Radii of Curvature of Samples Employed in Current Study

W/G Types	Length, l_1 [cm]	Length, l_2 [cm]	Curvature Radius, R [cm]
Rod (r = 2.5 mm)	101	72	3, 5
Tube (r_1 = 1.0 mm, r_2 = 2.5 mm)	201	90	3, 5, 7
Tube (r_1 = 1.5 mm, r_2 = 2.5 mm)	200	90	3, 5, 7, 9

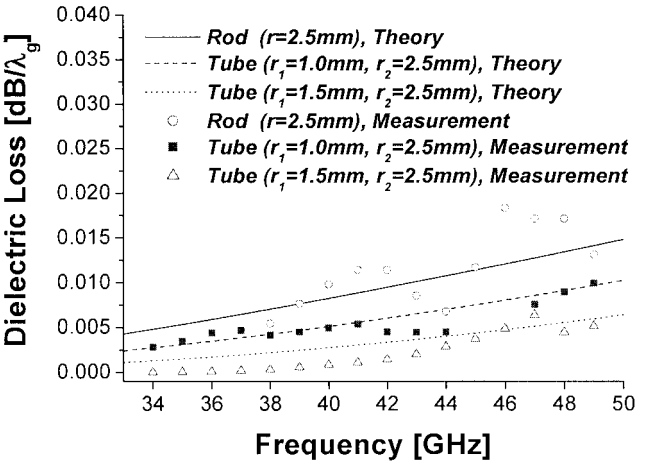

Figure 5 Dielectric losses of various flexible waveguides

the same curvature radius condition. In this case, the dielectric loss along the straight guide was assumed to be almost the same as that along the curved guide, as with radiation loss. Accordingly, the dielectric and radiation losses could be separated from the measured insertion losses. The radiation loss per unit angle, α_r for the rod and tube waveguides, was obtained from the difference between the dielectric loss and the measured insertion loss using Eq. (20).

$$\alpha_r = -\frac{10\,\mathrm{Log}_{10}[1-(10^{\alpha_d l_1/10}-10^{S_{21,l_1}/10})]}{180}\,[dB/Deg] \quad (20)$$

where α_d is the dielectric loss from (19) and S_{21,l_1} is the measured insertion losses.

In this experiment, the bent angle was fixed at 180°, regardless of any variations in the curvature radii. As such, the difference between the dielectric loss and the insertion loss, i.e., the radiation loss, was divided by the bent angle rather than the total angle in order to represent the radiation loss per unit angle.

6. RESULTS AND DISCUSSION

The dielectric losses, i.e., the attenuations per wavelength of the flexible dielectric waveguides, were determined from the measured insertion losses using Eq. (19). Figure 5 illustrates the dielectric losses for the rod and tube flexible waveguides relative to an operating frequency from 33 GHz to 50 GHz. The measured values of the dielectric losses for the rod and tube waveguides were below 0.02 dB/λ_g for the whole frequency range. In addition, the dielectric loss characteristics tended to increase slightly with the operating frequency. The experimental dielectric losses showed a relatively good agreement with the theoretical dielectric losses obtained using the perturbation method [14]. When determining the theoretical results, the loss tangent for the PTFE material was assumed to be 0.0001. A loss tangent for PTFE has rarely been observed in the Q-band and thus is obscure. For both the rod and tube waveguides, the dielectric losses increased relative to the frequency when more propagating power was confined in the dielectric region with an increase in the frequency from 33 GHz to 50 GHz, as illustrated in Figure 3. Furthermore, the dielectric loss for the rod waveguide was higher than that for the tube waveguide because the rod waveguide's dielectric area was larger than that of the tube waveguide.

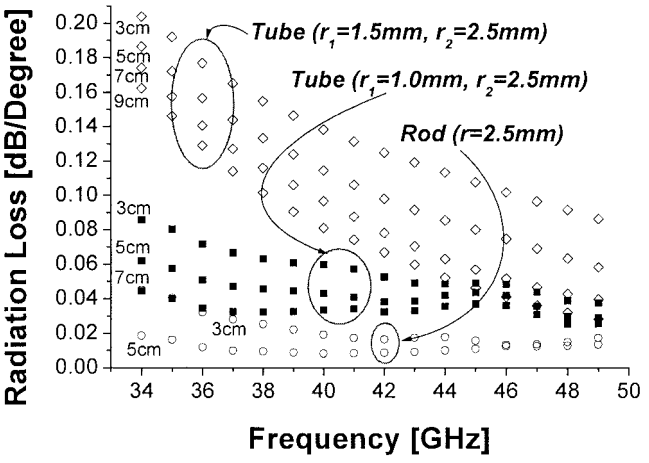

Figure 6 Radiation losses of various flexible waveguides

The radiation losses per unit angle for the rod and tube waveguides were determined using Eq. (20). The radiation loss per unit angle for the rod and tube waveguides with an operating frequency from 33 GHz to 50 GHz is shown in Figure 6. The radiation losses for the flexible waveguides, especially for the tube waveguide with an inner radius of 1.5 mm, decreased as the operating frequency increased from 33 GHz to 50 GHz. This tendency in the radiation loss for the tube waveguide is attributed to the increase in the propagating power confined within the waveguide in proportion to the variation of the frequency from 33 GHz to 50 GHz. The measurement results in Figure 6 also show that the radiation loss per unit angle decreased rapidly in proportion to the dielectric area, implying that the radiation loss for the rod waveguide was lower than that for the tube waveguide. In the case of the same type of flexible waveguide, the guided power was reduced as the radius of the curvature decreased. This means that the power radiated to the free space increased with an increase in the radius of the curvature. For the rod and tube waveguides, the radiation loss showed an opposite tendency in the dielectric loss because the radiated power was inversely proportional to the power confined in the dielectric region, as shown in Figure 3(c). Since the propagation constant of the second mode in Figure 2 was small, compared with that of the fundamental mode, the effects of the second mode on the dielectric and radiation losses of the fundamental HE_{11} mode were not distinct here.

5. CONCLUSION

The dielectric and radiation losses of circular flexible PTFE rod and tube waveguides were measured relative to an operating frequency in the Q-band. The dielectric losses below 0.02 dB/λ_g were obtained for the rod and tube waveguides based on the difference in the insertion losses measured between the waveguide samples with different lengths. It was found that the increase in the frequency and the dielectric region caused the increase in the dielectric loss irrespective of the rod or tube waveguide. The radiation losses for the rod and tube waveguides, which cannot be predicted within the regime of a small curvature radius based on current theories, were also measured based on the difference between the dielectric loss and the measured insertion loss. It was observed that the increase in the frequency, dielectric region in the guiding cross section, and curvature radii caused the reduction of the radiation loss irrespective of the rod or tube waveguide.

ACKNOWLEDGMENT

This work was supported by grant No. R01-2000-00261 from the Basic Research Program of the Korea Science & Engineering Foundation.

REFERENCES

1. S.K. Koul, Millimeter Wave and Optical Dielectric Integrated Guides and Circuits, Wiley, New York, 1997.
2. J. Weinzierl, C. Fluhrer, and H. Brand, Dielectric waveguides at submillimeter wavelengths, Proc. 6th Int Conf Terahertz Electronics (1998), 166–169.
3. T. Katoh, T. Kashiwa, and H. Hoshi, Automated millimeter-wave on-wafer testing system, IEICE Trans Electron E82-C (1999), 1312–1317.
4. I.M. Boese and R.J. Collier, Measurements on millmeter wave circuits at 140 GHz, IEE Proc Sci Meas Technol 145 (1998), 171–176.
5. H.L. Vilkaitis, Flexible wave guide and method for making same, U.S. Patent No. 3,940,718, Feb. 1976.
6. J. Musil and F. Žáček, Microwave Measurements of Complex Permittivity by Free Space Methods and Their Applications, Elsevier, New York, 1986.
7. J.A. Arnaud, Transverse coupling in fiber optics, Part III: Bending losses, Bell System Tech J 54 (1974), 1379–1394.
8. L. Lewin, Radiation from curved dielectric slabs and fibers, IEEE Trans Microwave Tech, MTT 22 (1974), 718–727.
9. K. Yammamoto, A novel low-loss dielectric waveguide for millimeter and submillimeter wavelengths, IEEE Trans Microwave Tech MTT 28 (1981), 580–585.
10. W.M. Bruno and W.B. Bridges, Flexible dielectric waveguides with powder cores, IEEE Trans Microwave Tech MTT 36 (1988), 882–890.
11. J. Obrzut and P.F. Goldsmith, Flexible circular waveguides at millimeter wavelengths from metallized Teflon tubing, IEEE Trans Microwave Tech MTT 38 (1990), 324–327.
12. A.S. Jazi and G.L. Yip, Classification of hybrid modes in cylindrical dielectric optical waveguides, Radio Science 12 (1977), 603–609.
13. M.M. Kharadly and J.E. Lewis, Properties of dielectric tube waveguides, Proc IEE 116 (1969), 214–224.
14. S. Ramo, J.R. Whinnery, and T.V. Duzer, Fields and waves in communication electronics, 3rd Ed., Wiley, New York, 1993.

ANALYSIS OF ELECTROMAGNETIC SCATTERING FROM PERIODIC STRUCTURES BY FEM TRUNCATED BY ANISOTROPIC PML BOUNDARY CONDITION

Suomin Cui[1] and Daniel S. Weile[1]
[1] Department of Electrical & Computer Engineering
University of Delaware,
Newark, DE 19716

Received 11 April 2002

ABSTRACT: *A method is presented for modeling open periodic structures by using the finite element method truncated by an anisotropic perfectly matched layer (PML). The method can be used to simulate periodic structures with inhomogeneous profile and arbitrary geometries. The PML is shown to be an effective method for mesh termination, even in the presence the grazing and evanescent fields generated by periodic structures. Numerical analysis is conducted for validation and to demonstrate the effectiveness of the proposed method.* © 2002 Wiley Periodicals, Inc. Microwave Opt Technol Lett 35: 106–110, 2002; Published online in Wiley InterScience (www.interscience.wiley.com). DOI 10.1002/mop.10530

Key words: *FEM; PML; periodic structures*